SUPPLEMENTAL INFORMATION

SUPPLEMENTAL FIGURES

Zanin et al. Figure S1 (Related to Figure 1)

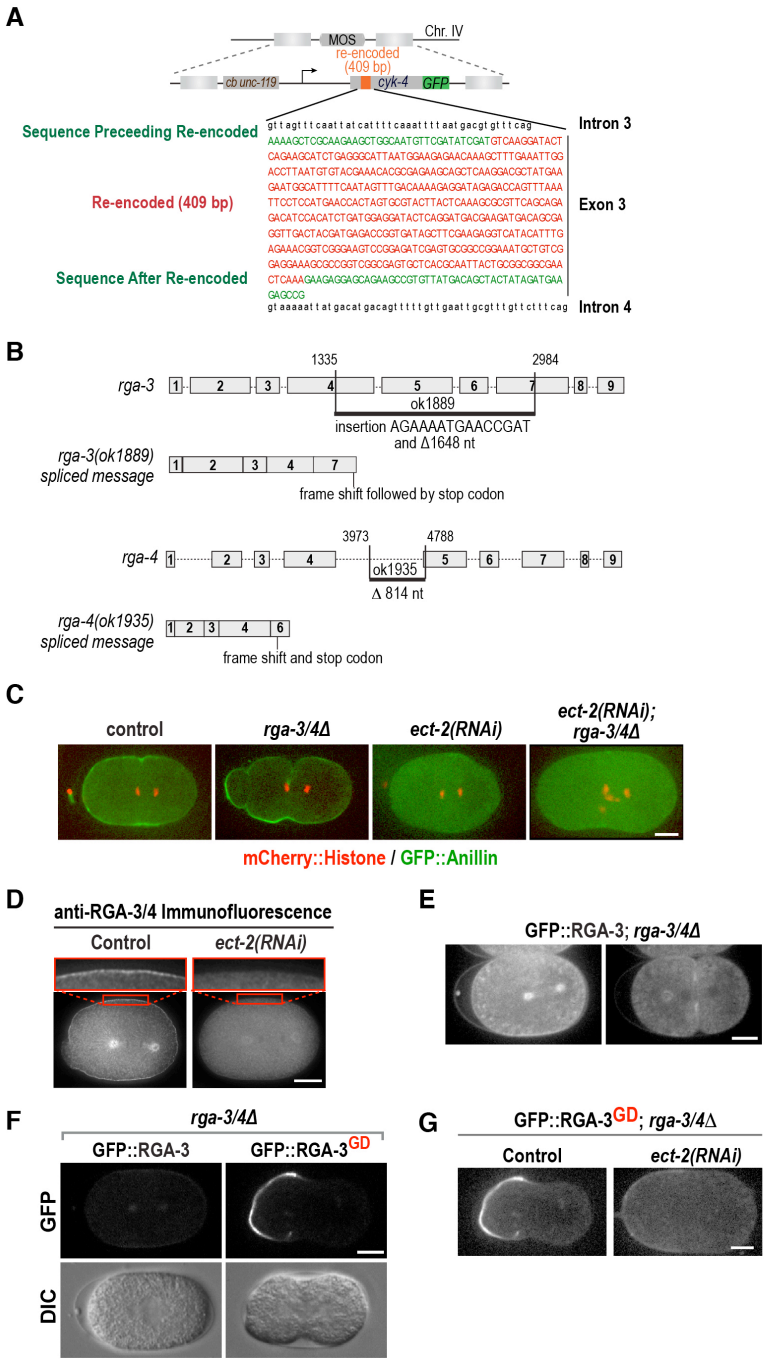

Zanin et al. Figure S2 (Related to Figure 2)

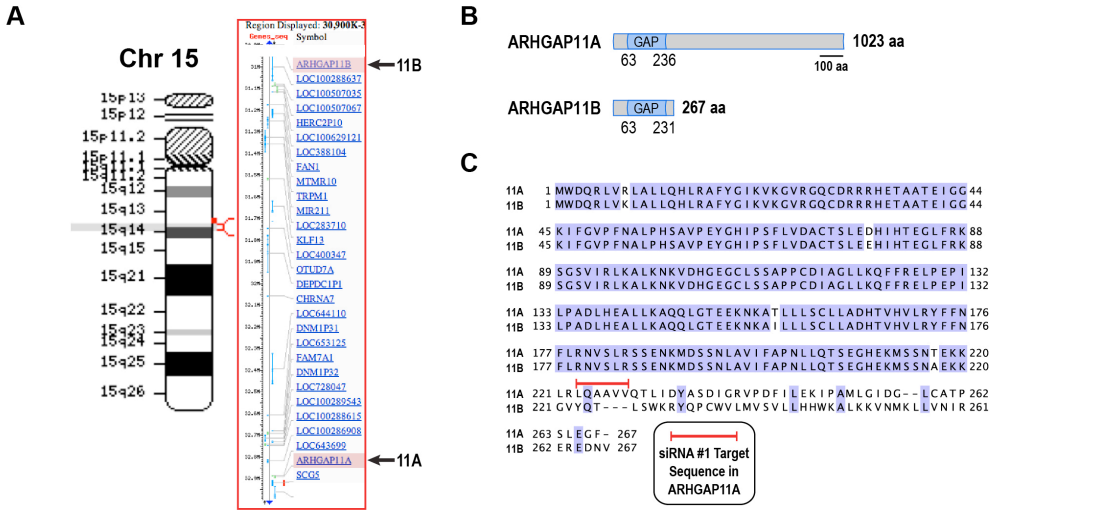

D

Species	Common Name/Descriptor	Length (aa)	GAP Domain START	GAP Domain END	Other Predicted Domains?	Accession #
Homo sapiens	Human	1023	63	236	NO	Q6P4F7
Xenopus laevis	African Clawed Frog	801	56	230	NO	NP_001089219.1
Danio rerio	Zebrafish	890	60	234	NO	NP_001180468.1
Strongylocentrotus purpuratus	Purple Sea Urchin	1342	66	238	NO	XP_003727009.1
Saccoglossus kowalevskii	Acorn Worm	1351	64	239	NO	XP_002740839.1
Anolis carolinensis	Green Anole/Carolina Anole	957	63	235	NO	XP_003214544.1
Oreochromis niloticus	Nile Tilapia	991	62	236	NO	XP_003447861.1
Tribolium castaneum	Flour Beetle	766	64	236	NO	XP_974382.1
Anopheles gambiae	Malaria mosquito	1097	73	241	NO	EGK96971.1
Apis mellifera	Honey Bee	1011	70	239	NO	XP_396895.4
Bombus impatiens	Bumble Bee	1026	69	238	NO	XP_003489264.1
Solenopsis invicta	Red Imported Fire Ant	1007	70	239	NO	EFZ11320.1
Drosophila willistoni	Fruit Fly	816	59	225	NO	XP_002070227.1
Aedes aegypti	Yellow Fever Mosquito	1045	73	239	NO	XP_001662343.1
Nematostella vectensis	Starlet Sea Anemone	558	65	236	NO	XP_001634298.1
Trichoplax adherens	Placozoan	474	67	238	NO	XP_002107738.1
Monosiga brevicollis MX1	Choanoflagellate	356	70	243	NO	XP_001742478.1
RGA-3/4:						
C. elegans	N/A	1085	63	268	NO	NP_504503.1
B. malayi	(Cause of Lymphatic Filariasis)	989	26	225	NO	XP_001902753.1

E

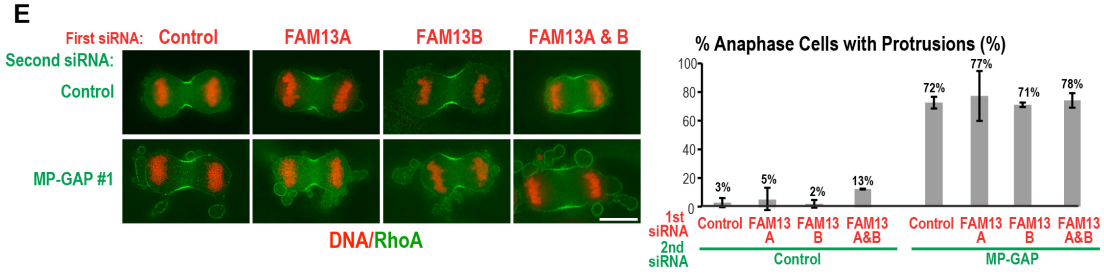

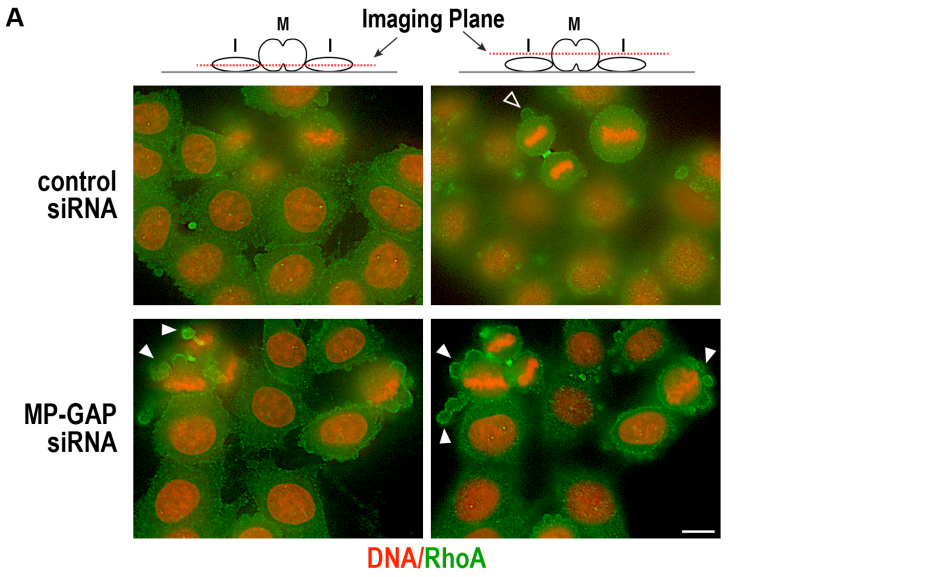
A
M
Imaging Plane
M
control siRNA
MP-GAP siRNA
DNA/RhoA
B
Time in Minutes from Mitotic Entry (Onset of Cell Rounding) to Anaphase
80
60
40
20
0
40 min
59 min
n=55
n=36
Control siRNA
MP-GAP siRNA
C
Time in Minutes
20
15
10
5
0
n=66
n=39
n=63
n=38
Time from Anaphase Onset to Cytokinesis Onset
Time from Anaphase Onset to Complete Furrow Ingression
Control siRNA
MP-GAP siRNA
D
Control siRNA
MP-GAP siRNA
DNA/Phalloidin

Zanin et al. Figure S4 (Related to Figure 4)

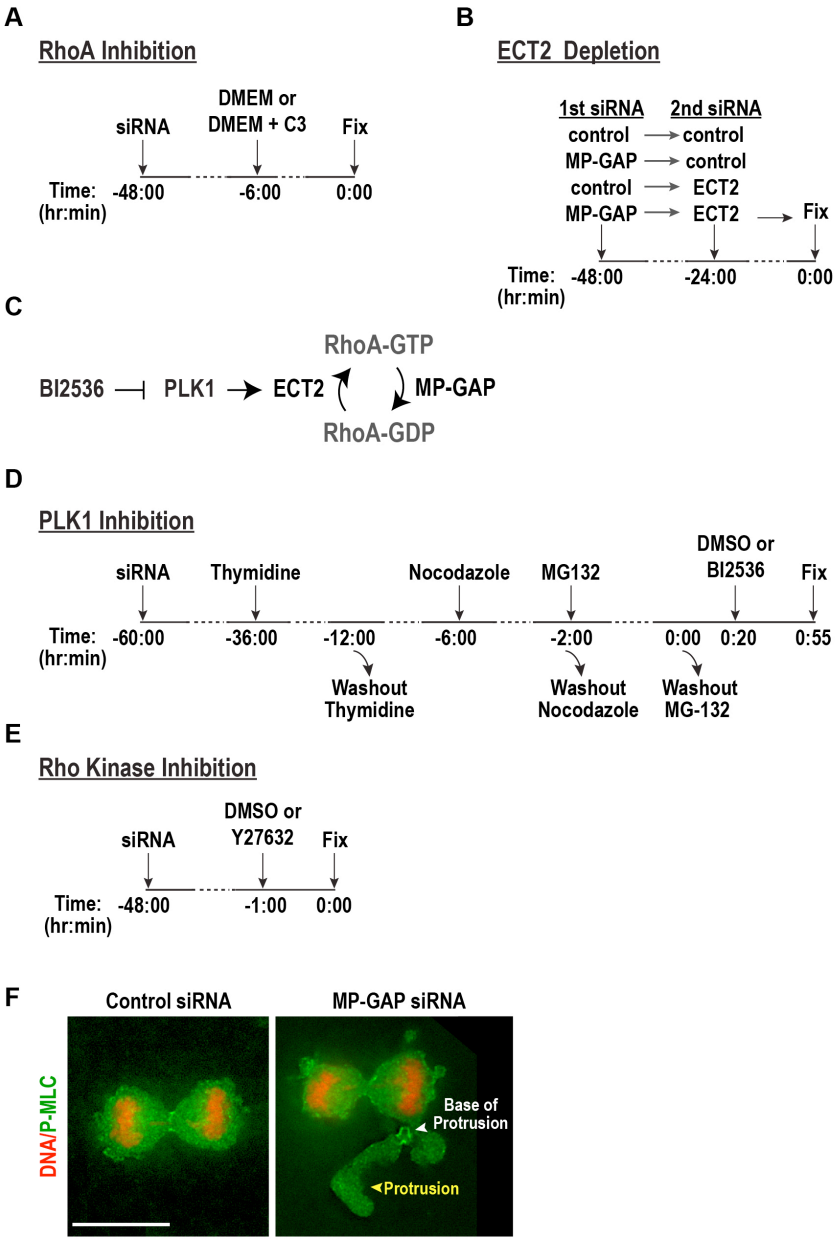

Zanin et al. Figure S5 (Related to Figure 6)

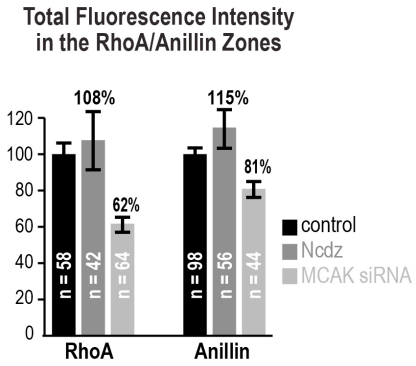

SUPPLEMENTAL FIGURE LEGENDS

Figure S1. Supplemental *C. elegans* data, related to Figure 1. (**A**) Schematic of the *cyk-4* MosSCI single copy transgene. The transgene was rendered resistant to RNAi targeting the endogenous locus by re-encoding the indicated region of exon 3 without altering the amino acid sequence or codon usage. (**B**) Schematic showing the locations of the *ok1889* and *ok1935* deletions in the *C. elegans rga-3* and *rga-4* genes and the predicted mutant spliced messages. In *ok1889,* the 1648 bp region between nucleotide 1335 and 2984 of *rga-3* is replaced by the sequence AGAAAATGAACCGAT, causing a premature stop codon in exon 7. In *ok1935*, an 814 bp region between nucleotide 3973 and 4788 of *rga-4*, including the first three nucleotides of exon 5, is deleted. Based on exon/intron predictions (NetGene2) exon 5 would not recognized resulting in splicing to exon 6, which would introduce a frame shift and a premature stop codon. The fact that the *rga-3/4Δ* mutant phenotype is as or more severe than the phenotype resulting from depleting RGA-3 and RGA-4 by RNAi, suggests that both deletions are null alleles. (**C**) Central plane fluorescence confocal images of control and *rga-3/4Δ* mutant embryos expressing GFP::Anillin and mCherry::Histone 120 seconds after anaphase onset. Depletion of ECT-2 by RNAi suppresses the GFP::Anillin accumulation and hypercontractility phenotypes exhibited by *rga-3/4Δ* mutant embryos. (**D**) Immunofluorescence images of anaphase one-cell stage wild-type (***left***) and *ect-2(RNAi)* (***right***) embryos stained with antibodies to RGA-3/4. Endogenous RGA-3/4 targets to the cortex and centrosomes in control, but not in *ect-2(RNAi)* embryos (>12 embryos were visualized for each condition). (**E**) Central plane fluorescence confocal images of a one-cell stage *rga-3/4Δ* mutant embryo expressing wild-type GFP::RGA-3 during metaphase (***left***) and cleavage furrow ingression (***right***). Like endogenous RGA-3/4 in fixed embryos (*see D*), GFP::RGA-3 localizes to the centrosomes, cortex and cleavage furrow. (**F**) Central plane fluorescence confocal (***top***) and DIC (***bottom***) images of mitotic one-cell embryos expressing wild-type or GAP-Defective

GFP::RGA-3 were acquired under identical imaging conditions. Compared to wild-type GFP::RGA-3, GAP-Defective GFP::RGA-3^{GD} is strongly enriched on the anterior cortex. (**G**) Central plane fluorescence confocal images of one-cell metaphase *rga-3/4Δ* embryos expressing GFP-RGA-3^{GD} were acquired either with (***right***) or without (***left***) depletion of the ECT-2 Rho GEF (>7 embryos were visualized for each condition). Bars, 10 μm.

Figure S2. The MP-GAP (ARHGAP11A) family, related to Figure 2. (**A**) Snapshot from the NCBI Map Viewer showing the location of ARHGAP11A and ARHGAP11B genes on human chromosome 15 (location 15q13.2). ARHGAP11B is a truncated version located ~2Mb from ARHGAP11A and is likely derived from a local duplication in this region (see *(B)* & *(C)* for domain structure and sequence comparisons). A non-homologous recombination event has been proposed to generate the truncated ARHGAP11B gene after the initial duplication event (Riley et al., 2002). Only ARHGAP11A is annotated as being present in other primates, mouse, rat, and lower vertebrate genomes, suggesting that the duplication and subsequent recombination leading to ARHGAP11B is evolutionarily recent in humans. (**B**) ARHGAP11A & ARHGAP11B protein schematics. GAP domain residue annotations are based on SMART (http://smart.embl-heidelberg.de/). (**C**) Primary sequence alignment of ARHGAP11B and the N-terminal region of ARHGAP11A. The red bracket indicates the sequence in ARHGAP11A targeted by the siRNA#1 used in all of the single oligo RNAi and rescue experiments. (**D**) List of members of the MP-GAP (ARHGAP11A) protein family, as well as two divergent representatives of nematode RGA-3. Selected MP-GAP family members from species spanning metazoan diversity are listed. The N-terminal location of the GAP domain and the absence of any other predicted domains is a consistent feature of family members. The predicted *Trichoplax*, sea anemone and choanoflagellate orthologs are shorter than the other family members. In the Drosophilids, only *D. willistoni* appears to have an MP-GAP ortholog. (**E**) Representative fluorescence images of HeLa cells stained

for DNA and RhoA after treatment with control, FAM13A pool, FAM13B pool, or FAM13A&B pool siRNA (First siRNA) along with control or MP-GAP #1 siRNA (Second siRNA). The mean percentage of anaphase cells with protrusions (>2 independent experiments) is plotted. Total number of cells analyzed: control siRNA (121 control siRNA, 171 MP-GAP siRNA), FAM13A siRNA (128 control siRNA, 106 MP-GAP siRNA), FAM13B siRNA (113 control siRNA, 104 MP-GAP siRNA), FAM13A and FAM13B siRNA (47 control siRNA, 61 MP-GAP siRNA). Error bars are the SD. Bars, 10μm.

Figure S3. MP-GAP is specifically required to suppress protrusion formation in mitotic cells, related to Figure 3. (**A**) Unsynchronized HeLa cells fixed and stained for DNA and RhoA 48 h after transfection with control (*top*) or MP-GAP (*bottom*) siRNAs. Images of two focal planes, one closer to the coverslip to visualize interphase cells (*left*), and a second central plane to visualize rounded mitotic cells (*right*), are shown. The open arrowhead marks a bleb, which are seen in control as well as ARHGAP11A siRNA treated cells, closed arrowheads mark large protrusions. (**B,C**) The timing of mitotic events was assessed in HeLa cells treated with control or MP-GAP siRNAs and filmed beginning 48 h after siRNA transfection. (**B**) MP-GAP siRNA treated cells took slightly longer than controls to progress from mitotic entry (defined as onset of cell rounding) to anaphase onset (student's t-test, $p<0.001$). Error bars are the 95% confidence interval. (**C**) The intervals from anaphase onset to the first bending of the cortex (cytokinesis onset) and from anaphase onset to the completion of cytokinesis were not affected by MP-GAP inhibition (n= number of cells scored, errors bars are the 95% confidence interval). (**D**) Unsynchronized HeLa cells were transfected with control or MP-GAP siRNA for 48 h and fixed and stained with Phalloidin. Filamentous actin is present on the cortex in protrusions induced by MP-GAP inhibition. Bars, 10μm.

Figure S4. Phosphorylated myosin light chain is enriched at the base of the protrusions induced by MP-GAP inhibition, related to Figure 4. (**A,B**) Schematics illustrating the experimental protocols used to inhibit RhoA through treatment with C3 (*A*) and Ect2 by RNAi (*B*). (**C**) Schematic illustrating how treatment with a PLK1 inhibitor blocks RhoA activation by preventing activation of the RhoGEF Ect2. (**D,E**) Schematics illustrating the experimental protocols used to inhibit PLK1 though treatment with BI2536 (*D*), and Rho Kinase by treatment with Y27632 (*E*). (**F**) Unsynchronized HeLa cells were transfected with control or MP-GAP siRNA for 48 h and fixed and stained with antibodies to phosphorylated myosin light chain (P-MLC). In addition to being concentrated at the cleavage furrow, P-MLC was strongly enriched at the base of the protrusions induced by MP-GAP inhibition. A requirement for myosin phosphorylation in protrusion formation could explain the potent suppression of protrusions observed following treatment with the Rho kinase inhibitor Y27632 (Fig. 4H) Bar, 10μm.

Figure S5. The total amount of RhoA and Anillin in the equatorial zone is reduced following MCAK inhibition, related to Figure 6. Graph of the total fluorescence intensity in the RhoA and Anillin zones in control, MCAK siRNA-treated, and low dose nocodazole-treated cells. n= number of linescans analyzed. Error bars are the SEM.

TABLES

Table S1: RNAi Phenotype of *C. elegans* RhoGAPs, related to Figure 1.

Sequence Name	Gene Name	Reported RNAi Phenotype
K08E3.6	*cyk-4*	embryonic lethal (3,6,7); sterile (4,5,10)
K09H11.3/Y75B7AL.4a,b	*rga-3/4*	embryonic lethal (3,6,7); escapers sterile (6)
2RSSE.1		wild type (11,**12 imaged n=8**)
BE0003N10.2	*chin-1*	wild type (3)
C01F4.2	*rga-6*	wild type (2,3,5)
C04D8.1	*pac-1*	wild type (1,3,4)
C16C2.3	*ocrl-1*	wild type (3,8)
C38D4.5	*tag-325*	wild type (1,2,3,4,5)
F12F6.5	*srgp-1*	wild type (3,4,5,7)
F23H11.4		wild type (1,3,4)
F35D2.5	*syd-1*	wild type (3,4,5)
F45H7.2	*gei-1*	wild type (1,3,4,5)
F47A4.3	*rcc-1*	wild type (1,3,4,5,6)
F56A6.2	*hum-7*	wild type (3,4)
H08M01.2	*rga-5*	wild type (3,4,5)
T04C9.1		wild type (1,3,4,5)
T23G11.5	*rlbp-1*	wild type (3,8)
W02b12.8	*rga-1*	wild type (3,4,6)
Y34B4A.8		wild type (3,5,**12**); embryonic lethal, reduced brood size, spindle position orientation defective, cleavage furrow initiation defective (11)
Y53C10A.4	*rga-2*	wild type (3,5,8,9)
Y92H12BL.4		wild type (3)
ZK669.1	*tag-341*	wild type (3,**12 imaged n=4**); embryonic lethal (4,5); reduced brood size (5)

1 Gonczy P et al., Nature 408:331-6. 2000
2 Fernandez AG et al., Genome Res 15:250-9. 2005
3 Sonnichsen B et al., Nature 421:231-7. 2003
4 Kamath RS et al., Nature 421:231-7. 2003

5 Rual JF et al., Genome Res 14:2162-8. 2004
6 Maeda I et al., Curr Biol 11:171-6. 2001
7 Piano F et al., Curr Biol 12:1959-64. 2002
8 Fraser AG et al., Nature 408:325-30. 2000
9 Simmer F et al., PLoS Biol 1:E12., 2003
10 Ceron J et al., BMC Dev Biol 7:30. 2007
11 Skop AR, et al., Science Jul 2;305(5680):61-6. 2004
12 This study. Embryonic lethality and filming of the first embryonic division were performed in cases where the knockdown phenotype was not certain based on prior work. For embryonic lethality tests, worms were singled at two different timepoints (24 and 48 hours post injection) and were allowed to lay embryos for 24 hours at 20°C. Adult worms were removed and hatched larvae and unhatched embryos were counted 24 hours later. First cell divisions were filmed 48 h after RNAi injection into OD95. n= number of embryos imaged.

MOVIE LEGENDS

Movie S1. ECT-2 depletion abolishes cortical contractility in the *C. elegans* embryo, related to Figure 1. The first division of wild-type (***left***) and *ect-2(RNAi)* (***right***) *C. elegans* embryos was filmed using DIC optics. ECT-2 depletion prevents RhoA activation and cleavage furrow formation. Images were acquired every 20 seconds. Playback is 120x realtime. Times are in minutes::seconds after the start of the sequence.

Movie S2. A GAP-Defective CYK-4 mutant results in phenotype similar to CYK-4 depletion, related to Figure 1. The first division of wild-type (***top, left***) or *cyk-4(RNAi)* embryos either carrying no transgene (***top, right***) or RNAi-resistant transgenes expressing wild-type CYK-4::GFP (***bottom, left***) or GAP-Defective CYK-4^{GD}::GFP (***bottom, right***) were filmed using DIC optics. Images were acquired every 20 seconds. Playback is 120x realtime. Times are in minutes::seconds after the start of the sequence.

Movie S3. A GAP-Defective RGA-3 mutant results in a phenotype similar to *rga-3/4Δ*, related to Figure 1. The first division of wild-type (***top, left***) or *rga-3/4Δ* mutant embryos either carrying no transgene (***top, right***) or RNAi-resistant transgenes expressing wild-type

GFP::RGA-3 (***bottom, left***) or GAP-Defective GFP::RGA-3^{GD} (***bottom, right***) were filmed using DIC optics. Images were acquired every 20 seconds. Playback is 120x realtime. Times are in minutes::seconds after the start of the sequence.

Movie S4. Mitotic entry in control and MP-GAP siRNA cells expressing Anillin::GFP, related to Figure 3. HeLa cells expressing Anillin::GFP that were transfected with control (***top***) or MP-GAP (***bottom***) siRNAs were followed from interphase into mitosis. Fluorescence and bright field images were acquired every 3 minutes. Playback is 6 frames per second. Times are in minutes::seconds after nuclear envelope breakdown (NEBD).

Movie S5. Anaphase in control and MP-GAP siRNA cells expressing Anillin::GFP, related to Figure 3. HeLa cells expressing Anillin::GFP that were transfected with control (***left***) or MP-GAP (***right***) siRNAs were followed from metaphase through telophase. Fluorescence and bright field images were acquired every 3 minutes. Playback is 6 frames per second. Times are in minutes::seconds after the last metaphase frame.

EXTENDED EXPERIMENTAL PROCEDURES

C. elegans strains used in this study

Strain no.	Genotype	Reference
N2	wild type (ancestral)	
OD769	*unc-119(ed3)III; ltSi195 [EZ-70; pcyk4::^{RR}cyk-4RE^{R459A}::gfp; cb-unc-119(+)] IV.*	This study.
OD770	*unc-119(ed3)III; ltSi196 [EZ-66; pcyk4::^{RR}cyk-4RE^{WT}::gfp; cb-unc-119(+)] IV.*	This study.
OD311	*rga-4(ok1935) unc-62(e644) rga-3(ok1988) V / nT1[qIs51] (IV;V).*	This study.
OD445	*rga-4(ok1935) rga-3(ok1988) V; ltSi25 [pOD928/EZ-36; prga-3::GFP::RGA-3^{WT}; cb-unc-119(+)] II.*	This study.
OD548	*rga-4(ok1935) rga-3(ok1988) V/nT1[qIs51](IV;V); ltIs44 [pAA173; pie-1/mCherry::PH(PLC1delta1); unc-119(+)]; ltIs37 [pAA64; pie-1/mCHERRY::his-58; unc-119 (+)] IV; ltSi64 [EZ-56; prga-3::GFP::RGA-3^{R88A}; cb-unc-119(+)] II*	This study.
OD296	*unc-119(ed3) III; ltIs37 [pAA64; pie-1/mCHERRY::his-58; unc-119 (+)] IV; ltIs28 [pASM14; pie-1/GFP-TEV-STag::ANI-1; unc-119 (+)]*	This study.
OD314	*unc-119(ed3) III; ltIs37 [pAA64; pie-1/mCHERRY::his-58; unc-119 (+)] IV; ltIs28 [pASM14; pie-1/GFP-TEV-STag::ANI-1; unc-119 (+)];rga-4(ok1935) unc-62(e644) rga-3(ok1988) V / nT1[qIs51] (IV;V).*	This study.
EG4322	*ttTi5605 II; unc-119(ed9) III.*	Frokjaer-Jensen et al., 2008
EG6250	*unc-119(ed3) III; cxTi10882 IV.*	Frokjaer-Jensen et al., 2008

The *C. elegans* strains used in this study are listed in the table above. The *rga-3(ok1889)* and *rga-4(ok1935)* single mutants (described in **Fig. S1B**) were crossed out four times against N2 and the *rga-3/4Δ* double mutant was balanced with nT1[qIs51](IV;V). In some strains, the *rga-3/4Δ* double mutant was marked with *unc-62(e644).* The *gfp::rga-3* transgenes were generated by introducing the GFP sequence into an engineered NotI restriction site after the start codon. The engineered wild-type and GAP-Defective

transgenes were cloned into pCFJ151 (Frokjaer-Jensen et al., 2008) and injected into strain EG4322 to obtain stable single-copy integrants (Frokjaer-Jensen et al., 2008). The *cyk-4::gfp* transgenes were generated by introducing the GFP sequence just before the stop codon. Exon 3 was re-encoded (**Fig. S1A**) to allow specific depletion of the endogenous protein by RNAi. The engineered wild-type and GAP-Defective mutant transgenes were cloned into pCFJ178 (Frokjaer-Jensen et al., 2008) and injected into strain EG6250 to obtain stable single-copy integrants. Transgene integration was confirmed by PCR of regions spanning each side of the insertion and by the presence of homogeneous GFP::RGA-3 and CYK-4::GFP fluorescence in all progeny.

C. elegans RNA-mediated interference

Oligonucleotides for *C. elegans* dsRNA production

Gene	Oligonucleotide 1	Oligonucleotide 2	Template	mg/mL
K08E3.6 (cyk-4)	CGTAATACGACTCACTATAGGTGTCAAAGACACTCAGAAAC	CGTAATACGACTCACTATAGGCCTCTTCGAATTGGCAGCAGC	N2 cDNA	1.0
RSSE.1	CGTAATACGACTCACTATAGGCAGTGGCGAGTTACAGTATGG	CGTAATACGACTCACTATAGGGTGAACATTCGATTCTCGTCG	N2 cDNA	3.1
Y34B4A.8	CGTAATACGACTCACTATAGGTGAGAAGCACTACAACAACG	CGTAATACGACTCACTATAGGCTAACTGTTATCCCCTCCG	N2 cDNA	1.0
ZK669.1 (tag-341)	TAGGAAGAGATGTTGTCTGCTCC	AATGTTCTGCTTGTGACACATTG	Kamath et al., 2003	4.5
T19E10.1A (ect-2)	TAATACGACTCACTATAGGTGGATCCGATTCTCGAACTT	AATTAACCCTCACTAAAGGACATTTGGCTTTGTGCTTCC	N2 genomic	1.8
Y51H4A.3 (rho-1)	TAATACGACTCACTATAGGTGGCTGCGATTAGAAAGAAG	AATTAACCCTCACTAAAGGCCTCACGAATTCCGTCCTTA	Kohara cDNA yk435f7	2.0
C09G12.8 (ced-10)	TAATACGACTCACTATAGGTCAAATGTGTCGTCGTTGGT	AATTAACCCTCACTAAAGGATCGCCTCATCGAAAACTTG	N2 cDNA	1.0
K03D3.10 (rac-2)	TAATACGACTCACTATAGGAAATGTGTCGTCGTTGGTGA	AATTAACCCTCACTAAAGGCTCGTTTGTGGTGTTTGTGG	N2 cDNA	1.2
R07G3.1 (cdc-42)	TAATACGACTCACTATAGGGATCAAGTGCGTCGTCGTT	AATTAACCCTCACTAAAGGGAGAATATTGCACTTCTTCTTCTTCTC	N2 cDNA	0.7

L4 hermaphrodites were injected with dsRNAs prepared by using the oligonucleotides listed in the table above to PCR-amplify regions from the indicated templates. Injected worms were incubated at 20°C for 20-28 h before dissection and imaging of their embryos (*cyk-4(RNAi)*, 23-27 h; *cdc-42, rac-2, ced-10,* and *ect-2(RNAi);* 20–24 h; *rho-1(RNAi)*, 24–28 h). For embryonic lethality tests, worms were singled 23-27 h post injection and were allowed to lay embryos for 24 h at 20°C. Adult worms were removed and hatched larvae and unhatched embryos were counted 24 h later.

Human cell culture and siRNA transfection

Cell Line	**Background**	**Description**	**Reference**
Gerlich #83	HeLa "Kyoto"	Expression of H2B-mRFP and MyrPalm-mEGFP.	Steigemann et al., 2009
MCP_ky_3367	HeLa "Kyoto"	Expression of MP-GAP-LAP(R6Kamp-LAP(GFP) from integrated BAC.	This study.
MCP_ky_2359	HeLa "Kyoto"	Expression of mouse Anillin-FLAP (R6Kamp-FLAP) from integrated BAC.	This study.
EZ1	HeLa "Kyoto"	Expression of human MP-GAP-LAP (R6Kamp-LAP(GFP) from integrated BAC, clonal cell line obtained by FACS.	This study.
EZ8	HeLa "Kyoto"	Expression of mouse Anillin-FLAP (R6Kamp-FLAP) from integrated BAC, clonal cell line obtained by FACS.	This study.
HeLa Flp-In T-Rex	HeLa	No transgene insertion	Tighe et al., 2004
HeLa Flp-In T-Rex (H2b:mRFP)	HeLa	H2b:mRFP	Tighe et al., 2004
EZ19	HeLa Flp-In T-Rex	Expression of Myc-LAP-^{RR}MP-GAP^{WT}	This study.
EZ20	HeLa Flp-In T-Rex	Expression of Myc-LAP-^{RR}MP-GAP^{R87A}	This study.

MCP_ky_2364	HeLa "Kyoto"	Expression of mouse Ect2-FLAP (R6 Kamp-FLAP) from integrated BAC.	Hutchins et al., 2010; Poser et al., 2008
EZ11	HeLa "Kyoto"	Expression of mouse Ect2-FLAP (R6 Kamp-FLAP) from integrated BAC, clonal cell line obtained by FACS.	This study.
EZ31	HeLa Flp-In T-Rex (H2b:mRFP)	Expression of Myc-LAP-RhoA^{WT} and H2b:mRFP	This study.
EZ53	HeLa Flp-In T-Rex (H2b:mRFP)	Expression of Myc-LAP-RhoA^{Q63L} and H2b:mRFP	This study.

The human cell lines used in this study are listed in the table above. To generate Anillin-FLAP and MP-GAP-LAP expressing cells lines, recombineering and stable transfection of the modified BACs were performed as described (Poser et al., 2008). Briefly, both a plasmid carrying two recombinases and the purified tagging cassette, were introduced into the *E. coli* strain containing the BAC vector using electroporation. Precise incorporation of the tagging cassette was confirmed by PCR and sequencing. The GFP-tagged BAC was isolated from bacteria using the Nucleobond PC100 kit (Macherey-Nagel, Germany). HeLa Kyoto cells were transfected with the isolated BACs using Effectene (Qiagen) and cultivated in selection media containing 400 µg/ml geneticin (G418, Invitrogen). The pool of HeLa cells stably expressing the GFP-tagged transgenes were analyzed by western blot and immunofluorescence using an anti-GFP antibody (Roche) to verify correct protein size and localization of the genes of interest.

HeLa cells were maintained at 37°C in a 5% CO_2 atmosphere in Dulbecco's modified Eagle's medium (Gibco or Biochromo) supplemented with 10% tetracycline-free fetal bovine serum (Clontech), 100 U/mL penicillin, 100 U/mL streptomycin and 2 mM L-glutamine unless stated otherwise. For immunofluorescence, HeLa cells were seeded on 12-mm poly-L-lysine coated coverslips in 12-well plates 24 h prior to transfection with siRNAs.

Human cell siRNAs used in the experiments in the paper

Gene	siRNA
Control	D-001810-01 (Dharmacon)
MP-GAP #1 (ARHGAP11A)	attacaggctgcagtagta, J-021122-05-0020 (Dharmacon)
ARHGAP11A pool	L-021122-00 (Dharmacon)
FAM13A pool	L-020516-00 (Dharmacon)
FAM13B pool	L-020738-01 (Dharmacon)
MCAK	GCAGGCUAGCAGACAAAU (Dharmacon) (Rankin and Wordeman, 2010)
Ect2	GGCGGAAUGAACAGGAUUU (Dharmacon) (Yuce et al., 2005)

Predesigned siRNAs (sequences listed above) were obtained from Dharmacon and used at a final concentration of 200 nM. A specific siRNA was chosen for ARHGAP11A (MP-GAP#1) and was used for all experiments. All siRNAs were transfected using Oligofectamine (Invitrogen) and reduced-serum Opti-MEM (Invitrogen) according to the manufacturer's instructions. The human RhoGAP screen in Fig. 2D was performed using Stealth siRNAs (Life Technologies) whose sequences are listed below.

refseq_gene_symbol (gene_id)	siRNA A	siRNA B	siRNA C	siRNA D
control	AGCUACACUAUCGA GCAAUUAACUU	UUCCUCUCCACGCGCAG UACAUUUA	GGAGUCACGCGAUCGU GACGCGCCA	
ECT2 (1894)	GGUCCAUCACAUGG GUGGAGUUAUU	GGACCACCAGUUGUAUU AAAUUGUU	CAGAUAUCUUUGAUGUA CACACUAA	CGACAUGUAGCUAACAC CAUUUGUA
KIF11 (3832)	GGAAACAGCCUGAG CUGUUAAUGAU	CCCAUCAACACUGGUAA GAACUGAA	CAUUCCCAGGAACUUUG CAAGUUAA	GAGAGCUCGGGAAGCUG GAAAUAUA
PLK1 (5347)	CCAUUGGGUGUAUC AUGUAUACCUU	GAAGAUGCUUCAGACAG AUCCCACU	GCCCAACCAUUAACGAG CUGCUUAA	GAGCUGCUUAAUGACGA GUUCUUUA
MKLP1 (9493)	CCACCUUUGCCGUC AUGCGAAAUUU	GCCAAACAGCUGGAGAU GCAGAAUA	GGAAGAGGUGCCGUUU GAUCCCAUA	CCUCGUUGUUUGGACAU GAUCUUUA
ARAP1(116985)	CCCACCGCAGGGAU CUUACAUCUAU	GACAGUAACAAGGACGC UUACUCUA	CAGGCUCAUGAGUGGG UCAAGUGUA	CAGAAACGAUGGGUGAG ACUGGAUA
ARAP2 (116984)	CCGAGCAACACUAG CAGCUAUCAUU	UGGGCCACAUUUGAAGU CAUUGAAA	GAGCGUCCUCUUCACUA CAAGGAAA	CACAGUCUGGCAUACUG CAAUUGAA
ARAP3 (64411)	CCUUCCCUAAGGGU GUGAUACCUUU	CCCUGUCCAUGUUCUUU CCAAUGAA	UGGCCACCCUCAUUGG GCAUCUCUA	GAUCAACCCUUUCUCUC CAAGUCAA
ARHGAP1 (392)	GGAUCCCUCGCCAA GUGCUCAAAUA	UGGAUGACACCAGCGAG GCUCUGAA	AGGAGAACUACCAGGUG CUUCGUUU	CCAGUACGUGGAGAGUG ACUACACA
ARHGAP4 (393)	GAGGUGGCUGAGAU CUGCGUUGAAA	ACAAGACUCUGAAGGCG ACACUGCA	CAGAGCAACACGUGGAG GUGGAUAA	CAGGAGACCGAAACCUU CUACCUCA
ARHGAP5 (394)	UAAACAGGGUUAGU CAGCAACAUAA	GAGUACGAAUUUGCAAC CAUAUAUA	GGUUGAUGCCAAAUCG CCUUACUUU	CAACCAUAAAGUGCCUC CACCUAUU
ARHGAP6 (395)	CCUUGCCUGCUGAG GCUCAAAGUAA	GGGAUAUUCCGAGUUG GAAGCUCAA	ACCGAUCCUGAUGUCG UGGACUAUU	CAGCCUGUUAGAGACCG AUCCUGAU
ARHGAP8 (23779)	CGGCUGCUGGAGUA UUUGAAGUACA	GACCAAUACGUUGAGAA CGAUUAUA	CGCAUACAAGGAGUUCG AUAGGAAA	AGUUUGGCGUCAGUCUG CAAUACCU
ARHGAP9 (64333)	CCAGGACAAGAAGG UCGGUUAGAUU	GGACAGUACUGAGUGG GAUGACAUU	CAGUGGUCCAGAAGCU UCGCUUUCU	CAGUACUGAGUGGGAUG ACAUUCAU
ARHGAP10 (79658)	GGAAAGGAAGCUCU GUCCCAUAGUU	CCAUCAUCCCAAGACCA GAAGGAAA	GAGAGAAAUUAUGGCAU UAAGUGUA	CAGUGCCGUUGAAACAC GAGGUAUA
ARHGAP11A/B	UGGCUGACCACACA	GAUCAUGGUGAAGGUU		

(9824/89839)	GUUCAUGUAUU	GCCUAUCUU		
ARHGAP11A (9824)			UAACUUUGAGCUGUUG CCAAGUAAU	UGGCAGAGAAGUAAAUG GAUGUUCU
ARHGAP12 (94134)	GGAUCAAGAGCUUC UUUCAUCGGAA	GGGUUGGUCAGAAGAG UUGGAUGAA	GGCAUACCUUAUAUACC AGUGACUA	GGCGGUGUUGCAGGGU UCAUCUUUA
ARHGAP15 (55843)	GGAAACACUGAAUU CUACCCGCCAA	UCAUAUUGGAUUGGUUC CACGCUAU	UCCACAUGGUCUACCAG AACCAGAU	CAGACUGCAUCACAGUG CUUCCGAU
ARHGAP17 (55114)	CCGAGUUCUAAUCA CUCAUUCCACA	CCGAAAUGCGAGCCCAU CAAGAUAA	CCCUAACUUGUUAUGG GCCAGAAAU	CAGAAGUCCUUAGUGAA GAUCUAUU
ARHGAP18 (93663)	GGACAAUUCCCAAG UUUAUUGUAAA	CCAUUAGAAUCAAGAAU CUUUGCCA	GGGUUAUAAAGUCAAAG CCAUUGUA	CAGGAUUCUUUGGAUGA ACUAUCUA
ARHGAP19 (84986)	GGGAGUGUGCGAGA UUGCACUAUUU	UCACUGCAAAUGACCUU CAGGAGAA	GAGCUGUUUCAACACGU UCAUGAUA	CGCGCUCCUUCAGUGGG CUUAUUAA
ARHGAP20 (57569)	CCGAGAGCCAAUGU UGUUCUCCUAA	GCCAGGACAGCUCUUU GGAAUUUCU	GGCCCAUUCUAAAGAUG AAGAUGUU	CAGGGACAGUCCUUCUG CUAGUGUU
ARHGAP21 (57584)	GAUAAUAAAGAAGC UGUCAUCCUAA	CAUAUGAUGAGGGUCU GGAUGAUUA	GGGAUCUAAUUAGUCGA AGAAUAAA	CGAGGGAAGUUUAACAU CAAGUUUA
ARHGAP22 (58504)	GAAGAAGGGAGUGC UGACCUGAGAA	GGAUGAAGUUCAGGCAU ACUCAAAU	ACCUAACAUUCUGCGGC CACAGGUA	GGGCACUCUGGAGUUG GCUAAACAA
ARHGAP23 (57636)	CAGGUCAUAGCUCU GAUCCAGAAUA	CAGGCCUUGUCACACUG GCUGUCAA	GGCCCAAGAGAUGGGU GCUCUCCUA	CCGCAAGACAGAUGAAC CUUGGAUU
ARHGAP24 (83478)	GCAACCACAGUGCA CUGCACAGUUU	GGAUAAAGAGCUUAGAA CAGCGAAA	GAAACUGGAGGAUACUG UUCGUUAU	CAGCAAGGAAGAGGAAG CAGGUGUU
ARHGAP25 (9938)	UGAAAUACAGCUGA ACUGUGCUGUU	ACAGGAGAACGAUGUCU CAAGACUU	CCUUGGAAGAAGAAGUC AAGGAAUU	UGGAGAAGAGGAAAUUG AUUCUUUG
ARHGAP26 (23092)	GAUAUCUGUGCUGA AUGGGAGAUAA	CCACUCAUGAUGUACCA GUUUCAAA	CCACACCGUUCAGUCAA CAGAGAAA	CAGGAACAAAGGAACAG CAUCAUCA
ARHGAP27 (201176)	GCCACCAUCCAGAA GCUACGCUAUA	GGGAGAAGGGCUACAU CAAAGACCA	UCAUCAGCACCUGGCAU AAGGCCAU	CAGAUGCUCUACACCAA CCACUUCA
ARHGAP28 (79822)	CCUCUCUCUUCCCU GUGGAAUAUAU	UCCGCCAUCUCUCUCUG AUUGAAUU	CAGGCCCUCAUGACAUU CUUCAAUA	GAGCUUCCAAGAGUUAU CAAGACAA
ARHGAP29 (9411)	GGAGUGACAACAAG CCUCCAGAUUA	UAGAUCUCUGGAUUCAG AAUCUAUA	CAGAUGCUCUAACAGUG CAGAUAUA	CAUGAUAUCUGUGACGU CUUGAAAU
ARHGAP30 (257106)	CCAAAGGACUGAGG CUCAAGGAGUU	CAGCCCAGUCCAGACGG CUGUCUAU	UAGCUGCCUGGAGCUC CCAUCUGAA	CAAUUGGAACCUGAGCG CUUGGUCA
ARHGAP31 (57514)	CCGAAGCUGUGCUU CUCCAUGAGAU	GCCAUUCCCAUUGCUGA CCUCUUCU	GCUCCUUGAGCUCUCAA CAUUUAAA	CGUUCUGGAUCAGACUC CAAAUCAA
ARHGAP32 (9743)	UCCAGUUCUUCUAG UUCCUAUUACA	CAGUGGAGAUCAGCCUC CUUCUUAU	CCAGCAGUUCAAAUUAU CAUUCCUU	CAGCCUCCAUGGGUCUU CGUUAUAA
ARHGAP33 (115703)	AGCUCUACUUCCGA GAGCUUCCGAA	UGCUCACCUACCAGCUC UAUGGGAA	GAGCUCCACCGAGGGU CCUUGUACA	CGGUGCAUAUUUGACCG GAGGUUCU
ARHGAP35 (2909)	UCAAGUAUGUCAUC UCUCACCUAAA	CAGCUCAAGUUUGUCUC CAAUCUCU	GGACAAUGCUGUCAUUC CAUACGAA	CAUUGUGGAGCAGACUG AAUUUAUU
ARHGAP36 (158763)	GCACUACUUUCUGA UCCAGUGGAAA	CCUUUCCAAUUGGCCAA CGACUUCU	GAGGAAGAUCCAGAGU GCACGCAUA	CCGCAGGACGAAGAUGG UAUCGAUA
ARHGAP39 (80728)	GGUGACCAGACAGA GGGCAUCUUCA	CCAGCUUCAUGGAGGG UGUGCUGUA	CCGACACUGAGAAAGCG CAGGAGUU	GCGAGUCCAUCAAGAAG CCCAUGAU
ARHGAP40 (343578)	GAGGGAAUAUCAAU GAGCAUCGCCU	CAGAACCCAACAGAAAU GCCUUAAA	UAGGAGACUUGUCCCU GCAGGAUAU	CACAAGACACCUGUCAG AGAUGUCA
ARHGAP42 (143872)	AGGACACGAGCAAU CUGCCUCUCUA	CAGCUGCAGUUCAACUU GCAGAAUA	GAACUUCUAUGAAGCAU CAUUAGAA	GAUUUAUACUCUGCCUG CCAUUAUA
ARHGAP44 (9912)	CCUCUGCCUCCAAA CUGAAGAAGCU	GCAAUUGCAGGAGCUUU GAAAUCUU	GACUCCCAGUAAUAUGG CAAUUGUU	CAGCUCUCAGCUGAUAU GUACAGUU
BCR (613)	CCUGGAGGUGGAUU CCUUUGGGUAU	UCCGCAUGAUCUACCUG CAGACGUU	CAGAAGAAGUGUUUCAG AAGCUUCU	CCAUCUUCUUCAAAGUG CCUGAGCU
CHN1 (1123)	GACUGAUGGCUUGA UUACUCUCUAU	GGCCCUGACCCUGUUU GAUACAGAU	GAGCACGUAGGAUACAC AACCUUAA	CAGAGAUGGUGAGAAGG CAGAUAUU
CHN2 (1124)	GCACCCUGACCACC CUGCAUGAUAU	CAUCACAUAUGAUACCU AUUCCAAA	CCCUUAAACUGUAUUUC AGAGACUU	CACACAACUUUAAGGUC CACACGUU
DEPDC1 (55635)	GCAAAUUGGCCAAG AAGCAAUGAUA	GAGGUCACUGAUGAUAC AUACCUUU	GCUGGAAGAUUAGUUU CUUUCUUAA	GAGAAGCAGUGGAUUGG CUUUAUGA
DEPDC1B (55789)	CGAAGUUCAUCAUC CAUAAUGUAUA	GAGUUAUUAGCUGCUAG AUUGGUAA	CACAGCUGCUAAUGUG GGCACUAAA	CCCUUUGGCCUUGCAGA CCUCUAUA
DEPDC7 (91614)	CCAGACCAAAUGGU GGUGGAAAUAA	CCGAACAGACUUAGUGA AAGAACUU	GCCAGGUAUGCAGAUG CAUUAUUUA	ACGUAUGUAUGGAGCAG CAUCAUAA
DLC1 (10395)	CCGCAAAGAGAAGU GUGUUUCACUA	GCACAAACAGAGGACUG CCAUUAUU	UCCUGAUCUGGAAUCAG GAUCUGAA	UGGACUCCAUGGUGCUG CUGAUUAU
FAM105A (54491)	UCCUGAGAAGUAUA CAGGCUCGAAU	GCAGAGGUUGAUUUACU CAGUUAUU	AGGGCACAAGCUGAAAU GGUGGAUU	GCUACUUCCGGAGGCUA CAUUUAUA
FAM13A (10144)	UCACACGAAGGAUU CAGAGCCUUAA	GCCCAGUGUUGAAGCCA CAUUGGAA	GAGGGCGAAACUGCUU CCUUCUUCA	ACCUUUCUAUUUGAGUG CUCAUGUA

FAM13B (51306)	GCAAGAUAUGUGAU UUGAAUGCCAA	GGAAGCAGAUGUUCCCU CAGCUAUU	GGAACAGUUUGAAAGG GAAAGAAAU	GAGCAAGAAAUAGUGAG CAGGAUAA
GMIP (51291)	UCAUCGUGCACUAC GAGCAGAUCUU	GGACGUGGCUGAAGAC ACCAAAGAU	ACGUCUCGAGUGUCCU CAAGCGAUU	CACACCUACCGAGAUUC CAACUCCA
HMHA1 (23526)	GCCAAGGUCAAAGC CUUCCAUUAUG	GAGGUGGAGCAGGACA ACAAGAUGA	CCUACUACCAGAUGAUG CAUAUGCA	GAGACGAUUGCUGUGGC CUUCAGUA
INPP5B (3633)	CAGGAACACGCUCU CUUCCUCUAUA	CAGAAAGAAGAGGAUUA CACCUAUA	CCAGCAUCUGCGUUGU GAAUUCUCA	GGGACCUCAACUACAGG AUAGAAGA
MYO9A (4649)	CCAGACUCGUUUAU CAGGAGCAUAA	GGGAAGCUCUUACUUU GGAUAUCAA	CCAACUCAGUCUUACAG CCACAAUU	CAACUUUCCACAGGCUA CAAAUCAA
MYO9B (4650)	UCAGCUCAAGCAGC CUGAAGAUUAU	CAGGCGGACUUUGAUG ACCUGUGUA	CCGGACCAGAUACAUUC CGUGUACA	GAACCAUCAAGUACGUG CAUAUGCA
OCRL (4952)	CCGAAUUCUUUGGA GAGGAACAAAU	CCCAGCUUCCGAGAUGC CAUAGAAA	CCAAGGAGAUCUGGCU UCUAGUAGA	GCGAUGUCUUGACUCUG CUUAUGAU
OPHN1 (4983)	GAGCUCACACAGGA UUUCCUCCCAU	GCUGCCAAGUCUGACAA CCUGGAUU	GCGAGAGGCUCAAGUG UUAUGAGCA	GAGCUAAAUGAAGUGGG CUUCAAGU
PIK3R1 (5295)	UGAACAGCAUUAAA CCAGACCUUAU	UGGAAUGUUGGAAGCA GCAACCGAA	CCUACUACUGUAGCCAA CAACGGUA	GAGAUAUCUCGAGGGAA GAAGUGAA
PIK3R2 (5296)	AGCUUAAGGUCUAU CACCAGCAGUA	CCUCGGACAACAGAGAG AUCGACAA	GGACCUCCCAGGAGCU GCAGAUGAA	GCCGCGAGUAUGACCAG CUUUAUGA
PRR5-ARHGAP8 (553158)	GAGAACGAUUAUAC CAUCGUCUAUU	CCAGCUUCAUCAAGGUC CUGUGGAA	CAUCAGUCACAAGUUUG GGAAGAAA	GAGUUCGAUAGGAAGUA CAAGAAGA
RACGAP1 (29127)	GCCAAGAACUGAGA CAGACAGUGUG	UCUCUGGCUGUGACCG CACAGUAAA	CCACUAACCUAGGACGA CAAGGCAA	CCCUCCUCAGCAAAGUG GAUGAUAU
RALBP1 (10928)	CCUCAGAGCUGAGA UUGCUGAAAUU	GAGCUGGAAAUAAAGAA CAAUCAUU	GGAAGACUAUGAGCCUA ACACUGUA	CGGAGACUGAGAAAGUG CAGGAAUU
SH3BP1 (23616)	GGAGCAGGAGGUGA ACAAGAUGACA	GGACUCCUAUGCCAACU ACUUCAUU	CCUGCGUCAUGAUGCU GCUUUCUGA	GAGGACUCCUAUGCCAA CUACUUCA
SRGAP1 (57522)	CACCCAGAAUGGGC GUGCAGCUGAA	CCAGUCCAGGCAGAGCU CAUGCUCA	GGUGCAGGAUAUGGAU GAUACGUUU	CAGAGAAUAUUUGGAAG GCAGUAAU
SRGAP2 (23380)	CAGUCAACUGCUGG AAUCUCCUCUU	CAUCCAUGACCUAUCUG ACCUUAUU	CCAAGGACAUCUUUCAU GACCUGAU	AAACCAUCAUCAUCCAG CAUGAGAA
SRGAP3 (9901)	GCUGCAUCCGUUAC AUCAAUUUAUA	GCAAGGAGAUUGGCCU GCAGAUGCA	CCUCUCGCCUGUGAAC UGUUGGUAU	CAGAUCGAGGCUAUUGC CAAGUUUG
STARD13 (90627)	GGGUUCCCGCAAUA CGCUCAGUUAU	GGACCUUGUAGAACCUC UUUGCAGA	UGGCUGUCAAGAAUGAU CAUGAUUU	AGGCUGUCUUUGGCGUU CCUCUCAU
STARD8 (9754)	CAGGCCAGAUCAAC CUCCUGCACAA	CCAGGAUCCAGAACCUG CGUCAAAU	GGUGUGGAGCUGUACC ACUAUGUCA	GGUGUGGAGCUGUACCA CUAUGUCA
SYDE1 (85360)	GGUGACUUCGAAGA CGACUUCGAUG	ACCCGCACCUGAAUCUC AAAGACUU	GACAGUGCAGCGGUCU GCCUAUCUG	UCCUCAAGGAUUAUCUU CGAGAGUU
SYDE2 (84144)	CAAAGCAGCUUUAU GAGGCUGUAUU	CAAAGAAACGCAAUUGG CUAUAUCA	CCACCGCUGCUAAGAG GAAUGUUAU	CCGAUACCAUCUUGAUA CCAGUGUA
TAGAP (117289)	GAAUGUCAAUCAGA GGGUGAUAUCA	GGAAGCUACUUUCAAGC GACCUCUU	ACGCCAAUAAUAUGGAG ACACUAAU	CCUGUUGGCAUCAUGUG AGAGUGAA

Phylogenetic tree construction

The phylogenetic tree based on alignment of human GAP domain sequences (Fig. 2G) was constructed using Clustal W2 – Phylogeny (http://www.ebi.ac.uk/Tools/phylogeny/clustalw2_phylogeny/) with the Neighbor-Joining clustering option. GAP domains were identified from whole protein sequences using SMART (http://smart.embl-heidelberg.de). The tree image was generated using FigTree v1.3.1 (http://tree.bio.ed.ac.uk/software/figtree/).

Light microscopy

The images of *C. elegans* embryos in Figures 1E,H and S1E-G were acquired at 20°C using an inverted Zeiss Axio Observer Z1 system equipped with a Yokogawa spinning-disk confocal head (CSU-X1), a 63x 1.4 NA Plan Apochromat objective, and a QuantEM:512SC EMCCD camera (Photometrics). Acquisition parameters, shutters, and focus were controlled by AxioVision software (Zeiss). Since *rga-3/4Δ* mutant embryos were partially osmosensitive, *rga-3/4Δ* and control embryos were filmed without pressure in osmotic support medium. Worms were dissected to release their embryos in a 4µl drop of L-15 blastomere culture medium (Edgar, 1995) on a 24x60mm coverslip mounted on a metal holder (Monen et al., 2005). A ring of Vaseline was placed around the drop, and the chamber was sealed with an 18 x 18 mm coverslip to prevent evaporation.

HeLa cells were seeded in a 35-mm glass-bottom dish coated with poly-D-lysine (MatTek) or Nunc Lab-Tek^{TM} chambered coverglass. Prior to filming, the medium was replaced with CO_2-independent medium (Life Technologies) supplemented with 10% fetal bovine serum, 100 U/mL penicillin, 100 U/mL streptomycin, and 2 mM L-glutamine. The medium was covered with mineral oil and cells were maintained between 35 and 37°C using a heated stage. Images in Figures 3C, 5B and S1C were acquired using a spinning disk confocal mounted on an inverted microscope (TE2000-E; Nikon) equipped with a 60x 1.4 NA Plan Apochromat lens (Nikon), a solid-state laser combiner (Andor Technology) with 491- and 561-nm lines, a CSU10 head (Yokogawa), and a high-resolution interline charge-coupled device camera (Clara; Andor Technology). Acquisition parameters, shutters, and focus were controlled by iQ 1.10.0 software (Andor Technology). Images in Figures 2A, 3F,G and 6G,H were acquired using an UltraVIEW VoX spinning disk microscope (PerkinElmer) attached to an Axio Observer D1 stand (Carl Zeiss, Inc.), equipped 63x 1.4 NA Plan-Apochromat oil immersion objective and 488 nm laser line. Immuofluorescence images of fixed cells in Figures 1G, 2F, 3A, 4B,D,G, and 5F were acquired using a

deconvolution microscope (DeltaVision; Applied Precision) equipped with a charge-coupled device camera (CoolSnap; Roper Scientific) and a 100X 1.3 NA U-Plan Apochromat objective (Olympus). Immunofluorescence images in Figure 6A,D were acquired on a Leica DMI6000B microscope with a 63x 1.4 NA objective and 1.6X additional magnification using an OrcaR2 (Hamamatsu) camera and Volocity acquisition software (PerkinElmer). Z stacks with a 0.5 μm image spacing were acquired using a Piezo Z stage (Mad City Labs) and exported as TIFFs for analysis. Immunofluorescence images in Figure 4E,F,H, S2E, S3A,D, 4SF were acquired on an Axioskop 2 microscope (Carl Zeiss, Inc.) equipped with a 100x 1.3 NA Plan-Neofluar oil immersion lens and a charge-coupled device camera (1300; Micromax) and controlled by MetaMorph software. All fixed cell images were computationally deconvolved using SoftWorx software (Applied Precision). Images were cropped and scaled and color overlays were generated in Adobe Photoshop. Figures were constructed in Adobe Illustrator.

Immunofluorescence

Immunofluorescence of *C. elegans* embryos was performed as previously described (Desai et al., 2003; Oegema et al., 2001) using a 20 minute methanol fixation and rabbit-anti RGA-3/4 (Schonegg et al., 2007; 1 μg/ml), mouse-anti α-tubulin (DM1-α; Sigma-Aldrich; 1:1000), and 1 μg/ml Hoechst. For staining of HeLa cells for RhoA and DNA, cells were fixed in 10% trichloroacetic acid (TCA) as previously described (Yonemura et al., 2004) prior to staining with mouse-anti RhoA (26C4: sc-418; Santa Cruz Biotechnology; 1:50) and 1μg/ml Hoechst. For staining of HeLa cells for P-MLC and actin, cells were fixed in 4% formaldehyde at room temperature for 15 minutes prior to staining with anti-phospho myosin light chain 2 (Ser19) antibody (3671S, Cell Signaling, 1:100) or Alexa Fluor488 Phalloidin (A12379, Life Technologies) and 1μg/ml Hoechst. For the Plk1 and tubulin immunofluorescence, HeLa cells were fixed in methanol and washed and permeabilized

with TBST (150 mM NaCl, 50 mM Tris pH 7.5, 0.5% Triton X-100) as previously described (Yuce et al., 2005). Cells were incubated with mouse anti-Plk1 antibodies (Santa Cruz; 1:50), followed by goat anti-mouse Fab fragments (Jackson Immunoresearch; 1:50), then incubated with mouse anti-α-tubulin antibody (DM1-α, Sigma-Aldrich; 1:200), and secondary antisera (anti-mouse Alexa 568, Invitrogen; anti-goat Alexa 488, Cedarlane). HeLa cells expressing MP-GAP::GFP were fixed in -20°C methanol for 5 min at room temperature and permeabilized for 2 min with 0.1% Triton/PBS before staining with goat-anti GFP (Poser et al., 2008) 1:5000), mouse-anti α-tubulin (DM1-α; Sigma-Aldrich; 1:1000) and 1μg/ml Hoechst.

Image Quantification

All image quantification was done in ImageJ. For details on measurement of Anillin::GFP accumulation and the width of the RhoA/Anillin zone, see Experimental Procedures in the main text. The maximum cortical RhoA fluorescence intensity in fixed cells (Fig. 4D) was measured from 20 pixel wide linescans drawn perpendicular to the cortex after subtracting cytoplasmic background. Midzone length (Fig. 6B) was measured in fixed cells in early anaphase cells by performing a 50 pixel wide line scan from pole-to-pole across the chromosomes and measuring the distance between the two peaks of fluorescence intensity. The total RhoA and Anillin fluorescence intensity in the RhoA/Anillin zone (Fig. S5) was measured by summing up the fluorescence intensity in their respective zones.

Western Blots

Western blots were performed on whole-worm and HeLa cell extracts. Western blots were initially probed using 1 μg/mL of rabbit anti–GFP or rabbit anti-RGA-3/4 which were detected using an HRP-conjugated secondary antibody (1:4,000; GE Healthcare Life

Sciences). To control for loading, the same blots was subsequently probed for α-tubulin using the monoclonal DM1-α (1:1000 for whole-worm and 1:4000 for HeLa cells; Sigma-Aldrich) followed by an alkaline-phosphatase–conjugated anti–mouse secondary antibody (1:4000; Jackson ImmunoResearch Laboratories, Inc.).

Cell Synchronization and Drug Treatment

Stocks of MG132 (Sigma), BI2536 (Lenart et al., 2007; Steegmaier et al., 2007), Y27632 (Cayman Chemicals) and Blebbistatin (Sigma) were made in DMSO. Stocks of C3 Transferase cell permeable (Cytoskeleton, Inc.) were made in water. Drug treated cells were washed three to five times with medium when shifted into another medium or drug. For the BI2536 (Fig. 4G, S4D) and blebbistatin (Fig. 5E,F) experiments, cells were transfected with control or MP-GAP siRNAs before starting the synchronization procedure. For the synchronization, cells were treated with 2mM thymidine for 24 h, released for 6 h, arrested in mitosis by adding 50 ng/ml Nocodazole for 4 h, washed and transferred to medium containing 10μM MG132 for 2 h (Petronczki et al., 2007). For the PLK1 inhibitor experiments (Fig. 4G, S4D), synchronized cells were washed to release them into anaphase, 100nM BI2536 was added 20 minutes after release, and cells were fixed and stained ~35 minutes after inhibitor addition (late anaphase). For the blebbistatin experiments (Fig. 5E,F), synchronized cells were washed and directly released into 100μM Blebbistatin containing medium and stained ~50 minutes after inhibitor addition. For the C3 (Fig. 4E) and Y27632 (Fig. 4H) experiments, cells were treated with control and MP-GAP siRNA for 48 h. Medium containing DMSO or 10μM Y27632 was added for 1 h before fixation. DMEM (without FCS) and with and without 0.5μg/ml C3 was added for 6 h before fixation.

To compare cytokinesis failure rates in the Gerlich #83 (H2B-mRFP and MyrPalm-mEGFP) and EZ11 (Ect2::GFP) cell lines, cells were transfected with control or MP-GAP

siRNAs for ~24 h, then 2mM thymidine was added for 24 h. Live-cell imaging was started ~8 h after release from the single thymidine block.

In Vitro GAP Assay

The MP-GAP GAP domain (1-253aa) was cloned into pET28 and expressed in BL21 *E. coli.* Frozen cells were thawed in extraction buffer (50 mM Tris pH7.5, 500 mM NaCl, 0.5 mM TCEP, 5 mM Imidazole, 5% Glycerol, 1mM PMSF, 0.05% Tween, EDTA-free protease inhibitor cocktail) and lysed using a microfluidizer. The lysate was centrifuged at 42,000 g for 30 minutes and the supernatant was mixed with 50% Ni-NTA beads (Qiagen) and incubated at 4°C for 1 h. The Ni-NTA beads were washed with 50 mM Tris pH7.5, 500 mM NaCl, 0.5 mM TCEP, 75 mM Imidazole, 5% Glycerol, 0.05% Tween and the GAP domain was eluted with 50 mM Tris pH7.5, 500 mM NaCl, 0.5 mM TCEP, 300 mM Imidazole, 5% Glycerol, 0.05% Tween. The GAP domain was stored in 10% sucrose at -80°C and dialyzed into 50mM Tris, 150 mM NaCl, 1mM $MgCl_2$ prior to the GAP assay.

The GAP assay was performed with RhoGAP assay Biochem kit according in manufacturers instructions (BK105, Cytoskeleton, Inc.). RhoA, Cdc42 and Rac1 were incubated with GTP and the MP-GAP GAP domain for 20 min at 37°C. The reaction was terminated by adding CytoPhos and the production of free phosphate from GTP hydrolysis monitored by measuring the absorbance at 650 nm.

SUPPLEMENTAL REFERENCES

Ceron, J., Rual, J.F., Chandra, A., Dupuy, D., Vidal, M., and van den Heuvel, S. (2007). Large-scale RNAi screens identify novel genes that interact with the *C. elegans* retinoblastoma pathway as well as splicing-related components with synMuv B activity. BMC Dev Biol 7, 30.

Edgar, L.G. (1995). Blastomere culture and analysis. Methods Cell Biol 48, 303-321.

Fernandez, A.G., Gunsalus, K.C., Huang, J., Chuang, L.S., Ying, N., Liang, H.L., Tang, C., Schetter, A.J., Zegar, C., Rual, J.F., et al. (2005). New genes with roles in the *C. elegans* embryo revealed using RNAi of ovary-enriched ORFeome clones. Genome Res 15, 250-259.

Fraser, A.G., Kamath, R.S., Zipperlen, P., Martinez-Campos, M., Sohrmann, M., and Ahringer, J. (2000). Functional genomic analysis of *C. elegans* chromosome I by systematic RNA interference. Nature 408, 325-330.

Frokjaer-Jensen, C., Davis, M.W., Hopkins, C.E., Newman, B.J., Thummel, J.M., Olesen, S.P., Grunnet, M., and Jorgensen, E.M. (2008). Single-copy insertion of transgenes in *Caenorhabditis elegans*. Nat Genet *40*, 1375-1383.

Gonczy, P., Echeverri, C., Oegema, K., Coulson, A., Jones, S.J., Copley, R.R., Duperon, J., Oegema, J., Brehm, M., Cassin, E., et al. (2000). Functional genomic analysis of cell division in *C. elegans* using RNAi of genes on chromosome III. Nature 408, 331-336.

Hutchins, J.R., Toyoda, Y., Hegemann, B., Poser, I., Heriche, J.K., Sykora, M.M., Augsburg, M., Hudecz, O., Buschhorn, B.A., Bulkescher, J., et al. (2010). Systematic analysis of human protein complexes identifies chromosome segregation proteins. Science 328, 593-599.

Kamath, R.S., Fraser, A.G., Dong, Y., Poulin, G., Durbin, R., Gotta, M., Kanapin, A., Le Bot, N., Moreno, S., Sohrmann, M., et al. (2003). Systematic functional analysis of the *Caenorhabditis elegans* genome using RNAi. Nature 421, 231-237.

Lenart, P., Petronczki, M., Steegmaier, M., Di Fiore, B., Lipp, J.J., Hoffmann, M., Rettig, W.J., Kraut, N., and Peters, J.M. (2007). The small-molecule inhibitor BI 2536 reveals novel insights into mitotic roles of polo-like kinase 1. Curr Biol 17, 304-315.

Maeda, I., Kohara, Y., Yamamoto, M., and Sugimoto, A. (2001). Large-scale analysis of gene function in *Caenorhabditis elegans* by high-throughput RNAi. Curr Biol 11, 171-176.

Monen, J., Maddox, P.S., Hyndman, F., Oegema, K., and Desai, A. (2005). Differential role of CENP-A in the segregation of holocentric *C. elegans* chromosomes during meiosis and mitosis. Nat Cell Biol 7, 1248-1255.

Piano, F., Schetter, A.J., Morton, D.G., Gunsalus, K.C., Reinke, V., Kim, S.K., and Kemphues, K.J. (2002). Gene clustering based on RNAi phenotypes of ovary-enriched genes in *C. elegans*. Curr Biol 12, 1959-1964.

Poser, I., Sarov, M., Hutchins, J.R., Heriche, J.K., Toyoda, Y., Pozniakovsky, A., Weigl, D., Nitzsche, A., Hegemann, B., Bird, A.W., et al. (2008). BAC TransgeneOmics: a high-throughput method for exploration of protein function in mammals. Nat Methods 5, 409-415.

Rankin, K.E., and Wordeman, L. (2010). Long astral microtubules uncouple mitotic spindles from the cytokinetic furrow. J Cell Biol *190*, 35-43.

Riley, B., Williamson, M., Collier, D., Wilkie, H., Makoff, A. (2002). A 3-Mb map of a large Segmental duplication overlapping the alpha7-nicotinic acetylcholine receptor gene (CHRNA7) at human 15q13-q14. Genomics. 79:197-209.

Simmer, F., Moorman, C., van der Linden, A.M., Kuijk, E., van den Berghe, P.V., Kamath, R.S., Fraser, A.G., Ahringer, J., and Plasterk, R.H. (2003). Genome-wide RNAi of *C. elegans* using the hypersensitive *rrf-3* strain reveals novel gene functions. PLoS Biol 1, E12.

Skop, A.R., Liu, H., Yates, J., 3rd, Meyer, B.J., and Heald, R. (2004). Dissection of the mammalian midbody proteome reveals conserved cytokinesis mechanisms. Science 305, 61-66.

Steegmaier, M., Hoffmann, M., Baum, A., Lenart, P., Petronczki, M., Krssak, M., Gurtler, U., Garin-Chesa, P., Lieb, S., Quant, J., et al. (2007). BI 2536, a potent and selective inhibitor of polo-like kinase 1, inhibits tumor growth in vivo. Curr Biol 17, 316-322.

Yuce, O., Piekny, A., and Glotzer, M. (2005). An ECT2-centralspindlin complex regulates the localization and function of RhoA. J Cell Biol *170*, 571-582.